sensors

MDPI

Article

Indium Tin Oxide-Based Voltammetric Biosensor for the Detection of Antibodies Against the SARS-CoV-2 Virus Spike Protein

Greta Zvirzdine, Maryia Drobysh, Almira Ramanaviciene, Vilma Ratautaite, Sarunas Zukauskas, Migle Stanciauskaite, Ieva Plikusiene and Arunas Ramanavicius *

NanoTechnas—Center of Nanotechnology and Materials Science, Faculty of Chemistry and Geosciences, Vilnius University, Naugarduko Str. 24, 03225 Vilnius, Lithuania; greta.zvirzdine@ftmc.lt (G.Z.); mariadrobysh@gmail.com (M.D.); almira.ramanaviciene@chf.vu.lt (A.R.); vilma.ratautaite@ftmc.lt (V.R.); sarunas.zukauskas@ftmc.lt (S.Z.); migle.stanciauskaite@chgf.stud.vu.lt (M.S.); ieva.plikusiene@chgf.vu.lt (I.P.)
* Correspondence: arunas.ramanavicius@chf.vu.lt; Tel.: +370-600-32332

Abstract

This study aims to propose a plausible application of a novel electrochemical biosensing system for detecting antibodies against SARS-CoV-2 (anti-rS) in serum samples. The uniqueness of this study lies in the biosensor utilizing recombinant spike glycoprotein (SCoV2-rS) immobilized on an indium tin oxide (ITO) electrode modified with (3-aminopropyl)triethoxysilane (APTES). The electrochemical performance was evaluated using square wave voltammetry (SWV), demonstrating a linear relationship between the current density and anti-rS concentration. The limit of detection (LOD) was found to be 113 ng/mL (0.75 nM), and the limit of quantitation (LOQ) was equal to 338 ng/mL (2.25 nM). The reported electrochemical biosensor offers a straightforward and efficient method for evaluating the immune status of individuals who have recovered from COVID-19 and been vaccinated against this virus without the need for any redox probe.

Keywords: SARS-CoV-2 virus; recombinant spike protein; affinity interaction; immune complex formation; antigen–antibody binding; indium tin oxide (ITO) electrode; square wave voltammetry (SWV); ellipsometry

Academic Editor: Miroslav Pohanka

Received: 29 August 2025
Revised: 12 October 2025
Accepted: 29 October 2025
Published: 4 November 2025

Citation: Zvirzdine, G.; Drobysh, M.; Ramanaviciene, A.; Ratautaite, V.; Zukauskas, S.; Stanciauskaite, M.; Plikusiene, I.; Ramanavicius, A. Indium Tin Oxide-Based Voltammetric Biosensor for the Detection of Antibodies Against the SARS-CoV-2 Virus Spike Protein. *Sensors* **2025**, *25*, 6737. https://doi.org/10.3390/s25216737

1. Introduction

The Severe Acute Respiratory Syndrome Coronavirus 2 (SARS-CoV-2), the causative agent of Coronavirus Disease 2019 (COVID-19), continues to mutate and spread. Thus, the development of methods for the accurate and rapid diagnosis of COVID-19, as well as the monitoring of the immune status of recovered and/or vaccinated individuals, remains a pressing issue. SARS-CoV-2 is an enveloped virus with a lipid bilayer produced by the membrane of the host cell, consisting of the membrane, envelope proteins, and spike glycoprotein (SCoV2-S) [1]. The SCoV2-S are observed as projections from the envelope's exterior and are crucial for host cell identification, fusion, and viral entry [2]. The human immune system response to SARS-CoV-2 is largely mediated by antibodies, and the SARS-CoV-2-S is a prominent target for neutralizing antibodies [2,3].

Biosensors have been widely used for SARS-CoV-2 diagnostics, showing express, straightforward, and reliable recognition. Numerous studies have been dedicated to detecting the SARS-CoV-2 genome, structural proteins, and expressed antibodies against the

coronavirus employing biosensors [4]. These biosensors are mainly based on optical [5–8], field-effect transistor [9–11], colorimetric [12], surface plasmon resonance [13–16], and electrochemical methods of analysis [17]. Electrochemical biosensors are considered sensitive, simple to operate, rapid, and cost-effective. Methods such as electrochemical impedance spectroscopy [18–20], cyclic voltammetry (CV) [21–23], differential pulse voltammetry (DPV) [24–26], amperometry [27–29], and square wave voltammetry (SWV) [30,31] are generally used to obtain an analytical signal. CV is an effective technique for characterizing various electroactive species and correlating the current-potential properties of each engaged oxidation or reduction reaction. SWV is also used in biosensor design due to its high selectivity and sensitivity [32]. The can be utilized to analyze reversible and irreversible reactions, slow electron transfer reactions, and catalytic reactions [33]. Additionally, compared to other pulsed techniques, it can preserve electroactive particles [34]. As the consumption of electroactive particles is reduced, electrode surfaces tend to be less contaminated with non-electroactive products [33]. Applying SWV, there is no necessity to exclude oxygen from the analyte solution, as far as oxygen reduction is incorporated into the background flow [35]. In this method, the applied potential is more cathodic than that for the reduction of oxygen. Notably, SWV is a rapid technique. A complete voltammogram can be recorded within a few seconds, compared to 2–3 min for DPV. Additionally, SWV is more sensitive than DPV, as both forward and reverse currents are measured in the former, whereas only forward currents are measured in the latter [36].

Indium tin oxide (ITO) is considered one of the most widely applied transparent conductive oxide thin films in biosensor design, owing to its good electrical conductivity and optical transparency [37]. Immobilization of biorecognition elements on the ITO electrode surface is a crucial step in the design process of biosensors. Commonly, self-assembled monolayers (SAMs) are applied for the functionalization of the working surface. Owing to straightforward preparation steps, reproducibility, and stability, silane-based SAMs are widely used for the modification of ITO [38]. Here are examples of some silanization agents, namely, triethoxymethylsilane, (3-isocyanatopropyl) triethoxysilane [39], carboxyethylsilanetriol [40], 3-mercaptopropyl trimethoxysilane [41], and (3-aminopropyl)triethoxysilane (APTES) [42]. APTES consists of three hydrolysable ethoxy groups forming Si–O bonds on the top of the ITO electrode surface and a terminal NH_2 group providing binding with biomolecules, namely, proteins [43].

To date, several studies have focused on the development of biosensors utilizing ITO as a conductive substrate for immobilizing capture biomolecules or detecting target compounds in the diagnosis of COVID-19. Among them, there are spectroelectrochemical [44], impedimetric [45], and dual-gate oxide semiconductor thin-film transistor-based [46] systems for the detection of recombinant spike glycoprotein (SCoV-S); a photoelectrochemical immunosensor for the recognition of SARS-CoV-2 nucleocapsid protein [47]; and electrochemiluminescence detection of antibodies against SARS-CoV-2 [48].

In this work, we report an electrochemical biosensing system for the recognition of antibodies against SARS-CoV-2 in real samples. SCoV2-rS was used as a sensing biomolecule, immobilized on the ITO working electrode functionalized with APTES. The signal registration after interaction between SCoV2-rS and antibodies against SARS-CoV-2 (anti-rS) was performed by CV and SWV. The analytical performance of the system was evaluated by calculating the limits of detection (LOD) and quantification (LOQ).

2. Materials and Methods

2.1. Chemicals and Other Materials

Indium tin oxide (ITO) coated glass slides with surface resistivity of 12 Ω/cm^2 were purchased from Sigma-Aldrich (Saint Louis, MO, USA). Ethanol (EtOH)(99.9%,

CAS# 64-17-5), (3-aminopropyl)triethoxysilane (APTES) (≥98%, CAS# 919-30-2), Na_2HPO_4 (≥99.0%, CAS# 7558-79-4) and NaH_2PO_4 (≥99.0%, CAS# 7558-80-7) for preparing phosphate buffer (PBS) solution and glutaraldehyde solution (GA) (50% *w*/*w* H_2O, CAS# 111-30-8) were obtained from Sigma-Aldrich (Steinheim, Germany). Baltymas (Vilnius, Lithuania) synthesized the SARS-CoV-2 recombinant Spike protein (SCoV2-rS) [18]. A volunteer who received one dose of the Vaxzevria vaccine and tested positive for COVID-19 two weeks later provided serum samples containing antibodies against the SARS-CoV-2 spike protein (anti-rS) at a laboratory of Tavo Klinika, Ltd. (Vilnius, Lithuania) under the Lithuanian Ethics Law (confirmed by the Vilnius Regional Biomedical Research Ethics Committee). Deionized water was used to prepare the aqueous solution. For the preparation of protein and antibody solutions as well as for electrochemical measurements, 0.1 M PBS solution, pH 7.4, was used.

2.2. ITO Surface Modification with APTES

In order to activate the ITO surface [49], ITO slides were treated with argon plasma by Super Cool Sputter Coater Leica EM SCD050 (Leica Microsystems GmBH, Praha, Czech Republic) under a vacuum depth of ~0.1 mbar in 5 min. Furthermore, the slides were incubated in a 1% ethanol solution of APTES overnight at room temperature, resulting in the formation of ITO/APTES (Figures 1 and 2, stage 1). After incubation, the ITO/APTES slides were rinsed with EtOH and dried by heating to 40 °C for 30 min on a magnetic stirring hotplate from Heidolph MR Hei-Tec (Schwabach, Germany).

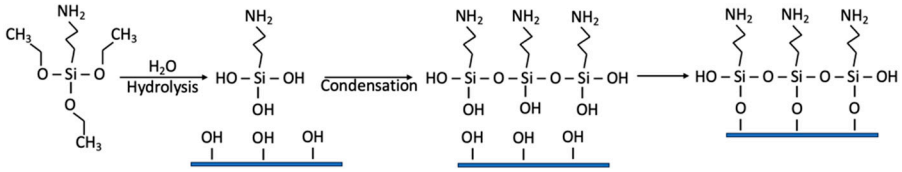

Figure 1. The APTES hydrolysis, condensation, and positioning on the ITO surface result in the formation of ITO/APTES. Adapted [50].

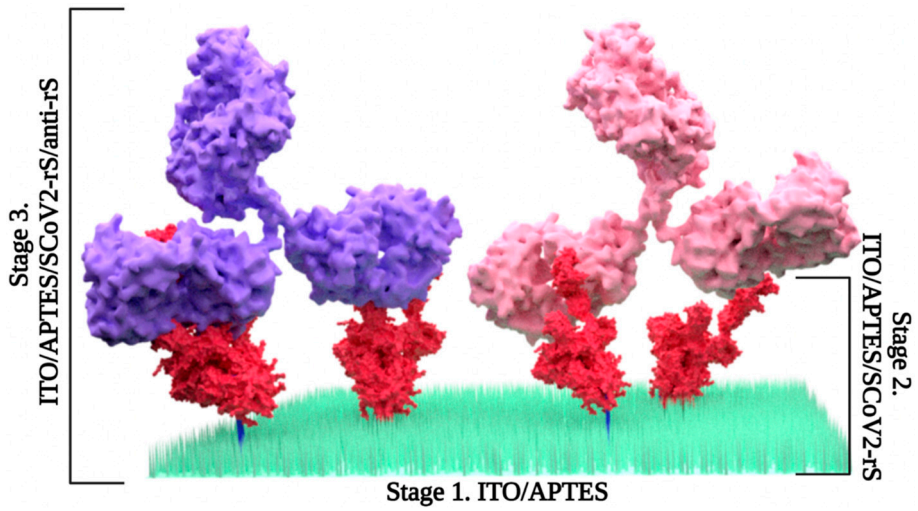

Figure 2. Schematic representation of the experimental stages. Stage 1—formation of SAM resulting in ITO/APTES; stage 2—incubation with SCoV2-rS with formation of ITO/APTES/SCoV2-rS; stage 3—anti-rS coupling resulting in ITO/APTES/SCoV2-rS/anti-rS formation.

2.3. ITO and ITO/APTES Surface Characterization

ITO and ITO/APTES electrode surfaces were characterized by means of electrochemical and optical methods, i.e., CV and ellipsometry. The electrochemical properties of ITO

and ITO/APTES electrodes were evaluated using a potentiostat, PalmSens4, controlled by PSTrace5 software, version 5.10.5604 (The Netherlands). The three-electrode electrochemical system consisted of ITO or ITO/APTES as the working electrode, the Ag/AgCl (3 M KCl) electrode as the reference electrode, and a platinum wire as the counter electrode.

Electrochemical measurements were performed to characterize the ITO and ITO/APTES surfaces in a 10 mL electrochemical cell containing a PBS solution, pH 7.4, and 2.5 mM of the redox probe $K_4[Fe(CN)_6]/K_3[Fe(CN)_6]$. The redox probe was used only for surface characterization measurements. Potential cycling was performed in the range from −0.1 V to +0.6 V at a scan rate of 0.1 V/s and a step size of 0.005 V. In total, 5 potential cycles were applied to characterize the surface. The 5th cycle was accepted as characteristic of the system.

The ellipsometric experiments were conducted using a rotating compensator-based ellipsometer, J. A. Woollam M2000X (Lincoln, NE, USA), operating in a spectral range from 210 nm to 1000 nm. The angle of incident light was fixed at 70 deg. Ellipsometric parameters Ψ and Δ dependence on wavelength were registered before and after modification using *N*-(3-aminopropyl)triethoxysilane (APTES, 99%).

2.4. Immobilization of SCoV-2

ITO/APTES were divided into nine separate sites with an area of 0.196 cm^2 by means of acrylic double-sided mounting tape placed on the top of the slide. Afterwards, each site was covered with 10 µL of 10 µg/mL SCoV2-rS in the PBS solution and left to air-dry for ~90 min. Furthermore, a custom-built construction with nine cells, each 400 µL in volume, was attached to the sticker. The next step was to covalently bind SCoV2-rS with ITO/APTES. For this purpose, ITO/APTES was placed in a 25 mL beaker with 25% GA solution and incubated in vapor for 15 min. After incubation in GA vapor, the resulting ITO/APTES/SCoV2-rS (Figure 2, stage 2) was kept in a 0.1 M PBS solution, pH 7.4, overnight at 2 °C.

2.5. Coupling with Anti-rS

ITO/APTES/SCoV2-rS was rinsed with 0.1 M PBS solution, pH 7.4, and dried with compressed air flow. Further, each cell was covered by 10 µL of anti-rS solution in a range of concentrations from 0 to 200 ng/mL, prepared in 0.1 M PBS solution, pH 7.4, in 10 min at room temperature, eventually forming ITO/APTES/SCoV2-rS/anti-rS (Figure 2, stage 3). After that, each cell was rinsed with 0.1 M PBS solution, pH 7.4, and electrochemical measurements were performed.

2.6. Electrochemical Measurements

The binding of the SCoV2-rS was evaluated in a three-electrode electrochemical cell consisting of an ITO-coated glass slide as the working electrode, an Ag/AgCl (KCl 3 M) electrode as the reference electrode, and a Pt wire serving as the counter electrode, with a volume of the electrochemical cell of 50 µL. SWV measurements were performed in a 0.1 M PBS solution, pH 7.4, by the µAUTOLAB TYPE III/FRA2 potentiostat (Metrohm, Barendrecht, The Netherlands) controlled by Nova software package version 2.1.6 from ECO-Chemie (Utrecht, The Netherlands). SWV signal was registered for ITO/APTES/SCoV2-rS/anti-rS formed after treatment with anti-rSpike in a concentration range from 0 to 200 ng/mL. SWV measurements were performed with the following parameters: a potential window from −0.6 to +0.3 V, a step size of 0.005 V, a modulation amplitude of 0.025 V, and a frequency of 20 Hz.

3. Results and Discussion

ITO and ITO/APTES electrodes were characterized by means of two electrochemical and optical methods, i.e., CV (Figure 3) and ellipsometry (Figure 4).

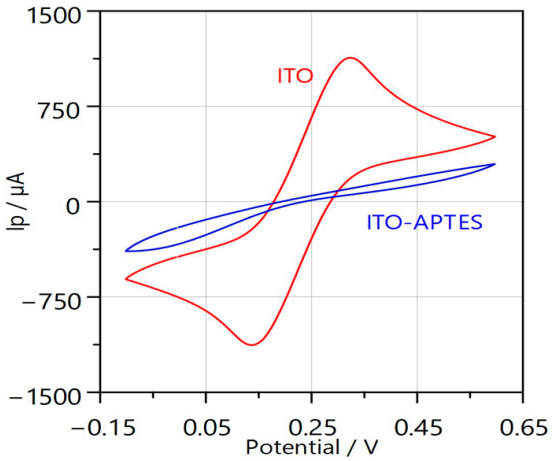

Figure 3. ITO and ITO/APTES surface characterization. Cyclic voltammetry-based surface characterization. CV was registered by potential cycling from −0.1 V to +0.6 V at a scan rate of 0.1 V/s and a step size of 0.005 V. In total, 5 potential cycles. This figure demonstrates the 5th potential cycle.

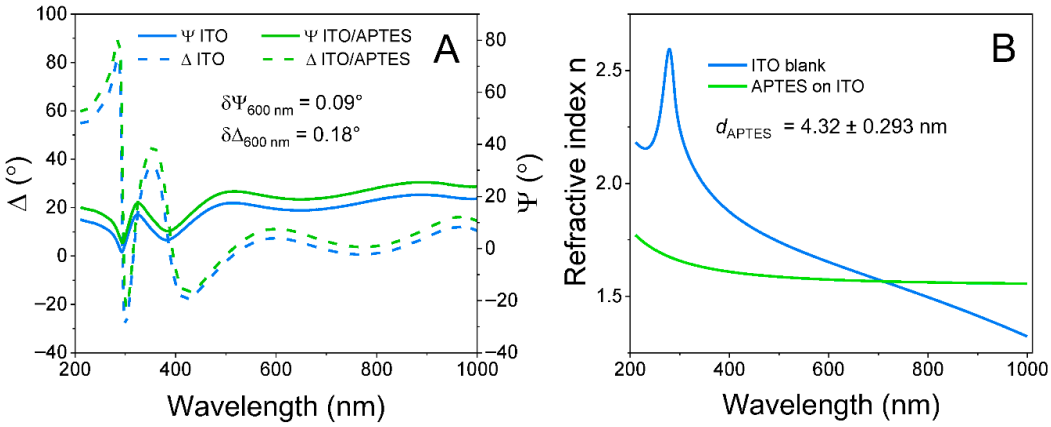

Figure 4. Ellipsometric measurement and modeling of ITO and APTES-functionalized ITO layers. (**A**) Ellipsometric parameter Ψ (solid line) and Δ (dashed line) shifts before ITO modification (blue) and after ITO/APTES modification (green). (**B**) Refractive index n of the ITO layer (blue) and the obtained APTES layer (green) derived from optical modeling of ellipsometric parameters.

The results are displayed in Figure 3, where the presence of APTES is shown to significantly reduce the sensor's conductivity. However, the presence of APTES serves to coat the electrode surface with $–NH_2$ groups, which are essential for protein immobilization on the surface.

The experimental curves in Figure 4A show ellipsometric parameters Ψ and Δ dependence on wavelength before and after modification using APTES.

Further, to determine the thickness of the formed APTES layer, an optical model based on regression analysis was applied. This model consisted of a glass substrate and a 168.97 nm ITO layer on top. The ITO layer in the optical model was characterized using ITO optical constants dispersion from the Complete EASE database. The ITO layer thickness was a free-fitting value. After that, the optical model was extended by adding an APTES layer on top of ITO. This layer was characterized using the Cauchy dispersion function with the following fixed parameters: A = 1.546, B = 0.010, and C = 0. The dispersion curves of the ITO and APTES refractive index are presented in Figure 4B. The thickness of the

APTES layer was a free-fitting value. After the fitting procedure, it was obtained that the APTES layer thickness was 4.32 nm, which is in good agreement with the literature [50].

Application of electrochemical and optical methods, i.e., CV and ellipsometry, gives interesting insights into the electrode surface properties. The electrochemical method clearly demonstrates that the ITO surface loses primary conductivity due to the APTES. However, the ellipsometric evaluation demonstrates that the layer thickness was only 4.32 nm.

The electrochemical performance of the ITO/APTES/SCoV2-rS/anti-rS biosensor was assessed using SWV across a range of anti-rS antibody concentrations from 0 to 200 ng/mL, as summarized in Table 1 and illustrated in Figure 5A. The measured current density (j) showed a clear increase with rising concentrations of anti-rS, indicating effective binding to the immobilized SCoV2-rS protein.

Table 1. Analytical data obtained from SWV detection of anti-rS.

[anti-rS], ng/mL	j, μA/cm^2
0	4.09 ± 0.98
20	3.48 ± 0.75
50	4.07 ± 0.41
100	5.17 ± 0.84
200	8.57 ± 0.69

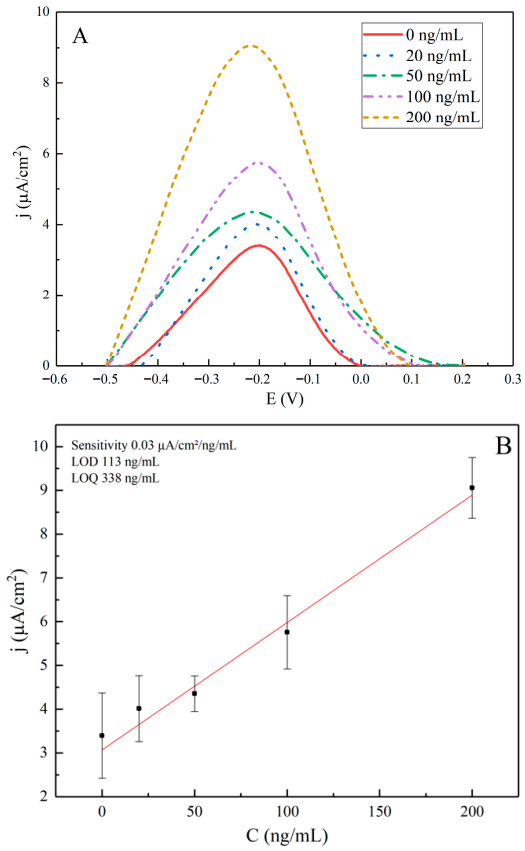

Figure 5. (**A**) Square wave voltammograms with baseline correction of ITO/APTES/SCoV2-rS/anti-rS in the range of concentrations from 0 to 200 ng/mL. Measurements were performed with the following parameters: potential window from −0.6 to +0.3 V, a step size of 0.005 V, a modulation amplitude of 0.025 V vs. Ag/AgCl(KCl_{3M}s), and frequency of 20 Hz in a 0.1 M PBS solution. The signal was normalized to the electrode area of 0.196 cm^2. (**B**) Calibration curves for SWV: current density (j) vs. anti-rS antibody concentration. Error bars represent standard deviations calculated from three independent measurements.

As shown in Figure 5A, the shapes of the SWV voltammograms differ slightly from each other, with a subtle shift in potential as the concentration of anti-rS antibodies increases. This trend reflects variations in antibody binding efficiency across the tested concentrations and possible inaccuracies during baseline corrections.

The calibration curve (Figure 5B) demonstrates a linear relationship between the j and the anti-rS concentration, with a high quality of linear fit (adjusted R^2 = 0.98). However, the error bars are quite broad, indicating variability in the measurements.

The calculated sensitivity of the sensor was determined to be 0.03 $\mu A/cm^2/ng/mL$, representing the response per unit increase in antibody concentration. The LOD and LOQ were calculated using the formulas LOD = 3.33 × SD/Slope and LOQ = 10 × SD/slope, where SD is the standard deviation of the blank sample ([anti-rS] = 0 ng/mL). The LOD was found to be 113 ng/mL, and the LOQ was determined to be 338 ng/mL. The relatively high values for LOD and LOQ reflect the variability in the standard deviations observed, which limits the sensor's ability to detect lower concentrations with high precision.

In our previous studies, we demonstrated that SCoV2-rS was covalently attached through primary amine functional groups on a gold surface, and the formed monolayer was stable and reproducible. Moreover, it has been proven that the impedimetric method and the applied experimental conditions, based on SCoV2-rS covalent coupling, are suitable for the further development of electrochemical biosensors for the serological diagnosis of COVID-19 [51].

The results obtained from the electrochemical characterization of the ITO/APTES/SCoV2-rS/anti-rS biosensor revealed relatively high SDs in j measurements, particularly for blank samples. These elevated SDs contributed to the high LOD observed in this study. A potential reason for this variability may stem from the electrode and biosensor design process, specifically during the surface modification and immobilization steps.

The activation of the ITO surface through argon plasma treatment and subsequent incubation with APTES aimed to enhance the formation of hydroxyl groups, thereby promoting better biorecognition. However, inconsistencies in this surface modification process, such as uneven distribution of APTES or incomplete formation of the SAM, could lead to variations in the binding sites available for immobilizing SCoV2-rS. This lack of uniformity could also explain the observed fluctuations in current density, leading to larger SDs and, consequently, a higher LOD.

Additionally, the biosensor's design, which incorporates ITO as the working electrode along with the APTES layer for protein immobilization, presents both advantages and challenges. While the choice of ITO provides optical transparency and good electrical conductivity, careful control of surface properties is essential to ensure reproducibility in measurements. The covalent binding of SCoV2-rS to the ITO/APTES surface via GA requires precise conditions to achieve optimal binding efficiency and minimize non-specific interactions.

While various electrochemical methods are available for detecting antibodies against SARS-CoV-2 (Table 2), the application of SWV with ITO electrodes specifically for this purpose is relatively uncommon. This makes our approach quite unique. In comparison to other SWV-based biosensors shown in Table 2, our LOD is higher (the conversion to nM was performed assuming the molecular weight of immunoglobulin G is approximately 150 kDa). For example, screen-printed carbon electrode (SPCE)-based sensors have achieved LODs as low as 47 pM for nucleocapsid protein as the sensing element. However, this method relies on the use of redox mediators. In contrast, our biosensor can detect SARS-CoV-2 antibodies directly from real serum samples without the need for redox mediators, thereby simplifying the measurement process. Furthermore, when comparing our findings to other ITO-based methods, such as those utilizing electrical resistive sensing or photoelectrochemical

techniques, our use of SWV for the direct detection of SARS-CoV-2 antibodies stands out as a not widely used approach with comparable LOD.

Table 2. Electrochemical biosensors have been previously reported for detecting antibodies against the SARS-CoV-2 virus.

Electrode	Sensing Element	Method	Redox Probe	LOD	
SPCE	Spike glycoprotein	CV, DPV	$[Fe(CN)_6]^{4-/3-}$	0.27 nM, 0.14 nM	[21]
SPCE	Spike glycoprotein	DPV	$[Fe(CN)_6]^{4-/3-}$	0.30 aM	[52]
SPCE	Spike glycoprotein	Electrochemical impedance spectroscopy (EIS)	-	0.42 nM	[53]
SPCE	Nucleocapsid protein	EIS, SWV	$[Fe(CN)_6]^{4-/3-}$	16 pM, 47 pM	[54]
SPCE	Nucleocapsid protein	Chronoamperometry	-	13 pM	[55]
Paper-based SPCE	Receptor-binding domain	SWV	$[Fe(CN)_6]^{4-/3-}$	6.40 pM	[56]
ITO	Spike glycoprotein	Electrical Resistive Sensing	-	~0.50 nM	[57]
ITO	Spike glycoprotein, Nucleocapsid protein	Photoelectrochemical	-	1.18 nM, 0.65 nM	[58]
ITO	Spike glycoprotein	SWV	-	0.75 nM	This study

Despite these strengths, the observed LOD of 113 ng/mL (0.75 nM) highlights a clear need for improvements. Future work should focus on optimizing the surface modification process, refining the electrode design, and exploring alternative strategies for antibody immobilization. By addressing these factors, we aim to enhance the sensitivity of our biosensor and lower the LOD, ultimately improving its applicability for rapid diagnostics.

4. Conclusions

In conclusion, the ITO/APTES/SCoV2-rS/anti-rS biosensor demonstrates potential for the direct detection of antibodies against SARS-CoV-2 in real serum samples, providing valuable insights into the evaluation of immune status after COVID-19 infection. The findings highlight the applicability of SWV, marking a unique contribution to the field of electrochemical immunosensors for monitoring concentration of antibodies specific to SARS-CoV-2 spike protein. Continued optimization of the biosensor design and surface modification processes will be essential to enhance sensitivity and improve LOD and LOQ, thereby improving its applicability in clinical settings.

Author Contributions: G.Z.: Investigation; data analysis. M.D.: investigation; data analysis; writing—original draft preparation. A.R. (Almira Ramanaviciene): writing—review and editing. V.R.: writing—review and editing. S.Z.: electrochemical measurements and data analysis. M.S. and I.P.: ellipsometric measurements and data analysis. A.R. (Arunas Ramanavicius): supervision; project administration; funding acquisition; conceptualization; methodology; writing—review and editing. All authors have read and agreed to the published version of the manuscript.

Funding: This research was supported by the Lithuanian Research Council project number S-MIP-24-111.

Institutional Review Board Statement: Not applicable.

Informed Consent Statement: Not applicable.

Data Availability Statement: The data presented in this study are available on request from the corresponding author.

Acknowledgments: The authors also wish to express their gratitude to the volunteer for his kind patience in enduring the painful blood collection procedures that made this study possible.

Conflicts of Interest: The authors declare no conflicts of interest.

References

1. Mittal, A.; Khattri, A.; Verma, V. Structural and antigenic variations in the spike protein of emerging SARS-CoV-2 variants. *PLoS Pathog.* **2022**, *18*, e1010260. [CrossRef]
2. Murin, C.D.; Wilson, I.A.; Ward, A.B. Antibody responses to viral infections: A structural perspective across three different enveloped viruses. *Nat. Microbiol.* **2019**, *4*, 734–747. [CrossRef]
3. Du, L.; He, Y.; Zhou, Y.; Liu, S.; Zheng, B.J.; Jiang, S. The spike protein of SARS-CoV—A target for vaccine and therapeutic development. *Nat. Rev. Microbiol.* **2009**, *7*, 226–236. [CrossRef]
4. Drobysh, M.; Ramanaviciene, A.; Viter, R.; Chen, C.-F.; Samukaite-Bubniene, U.; Ratautaite, V.; Ramanavicius, A. Biosensors for the determination of SARS-CoV-2 virus and diagnosis of COVID-19 infection. *Int. J. Mol. Sci.* **2022**, *23*, 666. [CrossRef]
5. Plikusiene, I.; Maciulis, V.; Ramanaviciene, A.; Balevicius, Z.; Buzavaite-Verteliene, E.; Ciplys, E.; Slibinskas, R.; Simanavicius, M.; Zvirbliene, A.; Ramanavicius, A. Evaluation of kinetics and thermodynamics of interaction between immobilized SARS-CoV-2 nucleoprotein and specific antibodies by total internal reflection ellipsometry. *J. Colloid Interface Sci.* **2021**, *594*, 195–203. [CrossRef]
6. Rabiee, N.; Fatahi, Y.; Ahmadi, S.; Abbariki, N.; Ojaghi, A.; Rabiee, M.; Radmanesh, F.; Dinarvand, R.; Bagherzadeh, M.; Mostafavi, E.; et al. Bioactive hybrid metal-organic framework (MOF)-based nanosensors for optical detection of recombinant SARS-CoV-2 spike antigen. *Sci. Total Environ.* **2022**, *825*, 153902. [CrossRef]
7. Gomez-Gonzalez, E.; Barriga-Rivera, A.; Fernandez-Munoz, B.; Navas-Garcia, J.M.; Fernandez-Lizaranzu, I.; Munoz-Gonzalez, F.J.; Parrilla-Giraldez, R.; Requena-Lancharro, D.; Gil-Gamboa, P.; Rosell-Valle, C.; et al. Optical imaging spectroscopy for rapid, primary screening of SARS-CoV-2: A proof of concept. *Sci. Rep.* **2022**, *12*, 2356. [CrossRef]
8. Plikusiene, I.; Maciulis, V.; Juciute, S.; Ramanavicius, A.; Balevicius, Z.; Slibinskas, R.; Kucinskaite-Kodze, I.; Simanavicius, M.; Balevicius, S.; Ramanaviciene, A. Investigation of SARS-CoV-2 nucleocapsid protein interaction with a specific antibody by combined spectroscopic ellipsometry and quartz crystal microbalance with dissipation. *J. Colloid Interface Sci.* **2022**, *626*, 113–122. [CrossRef]
9. Li, J.; Wu, D.; Yu, Y.; Li, T.; Li, K.; Xiao, M.M.; Li, Y.; Zhang, Z.Y.; Zhang, G.J. Rapid and unamplified identification of COVID-19 with morpholino-modified graphene field-effect transistor nanosensor. *Biosens. Bioelectron.* **2021**, *183*, 113206. [CrossRef]
10. Poghossian, A.; Jablonski, M.; Molinnus, D.; Wege, C.; Schoning, M.J. Field-Effect Sensors for Virus Detection: From Ebola to SARS-CoV-2 and Plant Viral Enhancers. *Front. Plant Sci.* **2020**, *11*, 598103. [CrossRef]
11. Hwang, M.T.; Park, I.; Heiranian, M.; Taqieddin, A.; You, S.; Faramarzi, V.; Pak, A.A.; van der Zande, A.M.; Aluru, N.R.; Bashir, R. Ultrasensitive Detection of Dopamine, IL-6 and SARS-CoV-2 Proteins on Crumpled Graphene FET Biosensor. *Adv. Mater. Technol.* **2021**, *6*, 2100712. [CrossRef]
12. Ventura, B.D.; Cennamo, M.; Minopoli, A.; Campanile, R.; Censi, S.B.; Terracciano, D.; Portella, G.; Velotta, R. Colorimetric Test for Fast Detection of SARS-CoV-2 in Nasal and Throat Swabs. *ACS Sens.* **2020**, *5*, 3043–3048. [CrossRef]
13. Wu, Q.; Wu, W.; Chen, F.; Ren, P. Highly sensitive and selective surface plasmon resonance biosensor for the detection of SARS-CoV-2 spike S1 protein. *Analyst* **2022**, *147*, 2809–2818. [CrossRef]
14. Liang, J.; Zhang, W.; Qin, Y.; Li, Y.; Liu, G.L.; Hu, W. Applying Machine Learning with Localized Surface Plasmon Resonance Sensors to Detect SARS-CoV-2 Particles. *Biosensors* **2022**, *12*, 173. [CrossRef]
15. Chen, Z.; Li, J.; Li, T.; Fan, T.; Meng, C.; Li, C.; Kang, J.; Chai, L.; Hao, Y.; Tang, Y.; et al. A CRISPR/Cas12a-empowered surface plasmon resonance platform for rapid and specific diagnosis of the Omicron variant of SARS-CoV-2. *Natl. Sci. Rev.* **2022**, *9*, nwac104. [CrossRef]
16. Jiang, M.; Dong, T.; Han, C.; Liu, L.; Zhang, T.; Kang, Q.; Wang, P.; Zhou, F. Regenerable and high-throughput surface plasmon resonance assay for rapid screening of anti-SARS-CoV-2 antibody in serum samples. *Anal. Chim. Acta* **2022**, *1208*, 339830. [CrossRef]
17. Kumar, N.; Shetti, N.P.; Jagannath, S.; Aminabhavi, T.M. Electrochemical sensors for the detection of SARS-CoV-2 virus. *Chem. Eng. J.* **2022**, *430*, 132966. [CrossRef]
18. Liustrovaite, V.; Drobysh, M.; Rucinskiene, A.; Baradoke, A.; Ramanaviciene, A.; Plikusiene, I.; Samukaite-Bubniene, U.; Viter, R.; Chen, C.-F.; Ramanavicius, A. Towards an electrochemical immunosensor for the detection of antibodies against SARS-CoV-2 spike protein. *J. Electrochem. Soc.* **2022**, *169*, 037523. [CrossRef]
19. Rashed, M.Z.; Kopechek, J.A.; Priddy, M.C.; Hamorsky, K.T.; Palmer, K.E.; Mittal, N.; Valdez, J.; Flynn, J.; Williams, S.J. Rapid detection of SARS-CoV-2 antibodies using electrochemical impedance-based detector. *Biosens. Bioelectron.* **2021**, *171*, 112709. [CrossRef]
20. Tabrizi, M.A.; Fernández-Blázquez, J.P.; Medina, D.M.; Acedo, P. An ultrasensitive molecularly imprinted polymer-based electrochemical sensor for the determination of SARS-CoV-2-RBD by using macroporous gold screen-printed electrode. *Biosens. Bioelectron.* **2021**, *196*, 113729. [CrossRef]
21. Drobysh, M.; Liustrovaite, V.; Baradoke, A.; Viter, R.; Chen, C.-F.; Ramanavicius, A.; Ramanaviciene, A. Determination of rSpike protein by specific antibodies with screen-printed carbon electrode modified by electrodeposited gold nanostructures. *Biosensors* **2022**, *12*, 593. [CrossRef]
22. Oliveira, M.E.; Lopes, B.V.; Rossato, J.H.H.; Maron, G.K.; Gallo, B.B.; La Rosa, A.B.; Balboni, R.D.C.; Alves, M.L.F.; Ferreira, M.R.A.; da Silva Pinto, L.; et al. Electrochemical Biosensor Based on Laser-Induced Graphene for COVID-19 Diagnosing: Rapid and Low-Cost Detection of SARS-CoV-2 Biomarker Antibodies. *Surfaces* **2022**, *5*, 187–201. [CrossRef]

23. Silva, L.R.G.; Stefano, J.S.; Orzari, L.O.; Brazaca, L.C.; Carrilho, E.; Marcolino-Junior, L.H.; Bergamini, M.F.; Munoz, R.A.A.; Janegitz, B.C. Electrochemical Biosensor for SARS-CoV-2 cDNA Detection Using AuPs-Modified 3D-Printed Graphene Electrodes. *Biosensors* **2022**, *12*, 622. [CrossRef] [PubMed]
24. Zhao, H.; Liu, F.; Xie, W.; Zhou, T.C.; OuYang, J.; Jin, L.; Li, H.; Zhao, C.Y.; Zhang, L.; Wei, J.; et al. Ultrasensitive supersandwich-type electrochemical sensor for SARS-CoV-2 from the infected COVID-19 patients using a smartphone. *Sens. Actuators B Chem.* **2021**, *327*, 128899. [CrossRef]
25. Yang, B.; Zeng, X.; Zhang, J.; Kong, J.; Fang, X. Accurate identification of SARS-CoV-2 variant delta using graphene/CRISPR-dCas9 electrochemical biosensor. *Talanta* **2022**, *249*, 123687. [CrossRef]
26. Hatamluyi, B.; Rezayi, M.; Amel Jamehdar, S.; Rizi, K.S.; Mojarrad, M.; Meshkat, Z.; Choobin, H.; Soleimanpour, S.; Boroushaki, M.T. Sensitive and specific clinically diagnosis of SARS-CoV-2 employing a novel biosensor based on boron nitride quantum dots/flower-like gold nanostructures signal amplification. *Biosens. Bioelectron.* **2022**, *207*, 114209. [CrossRef]
27. Raziq, A.; Kidakova, A.; Boroznjak, R.; Reut, J.; Öpik, A.; Syritski, V. Development of a portable MIP-based electrochemical sensor for detection of SARS-CoV-2 antigen. *Biosens. Bioelectron.* **2021**, *178*, 113029. [CrossRef]
28. Mojsoska, B.; Larsen, S.; Olsen, D.A.; Madsen, J.S.; Brandslund, I.; Alatraktchi, F.A. Rapid SARS-CoV-2 Detection Using Electrochemical Immunosensor. *Sensors* **2021**, *21*, 390. [CrossRef]
29. Fabiani, L.; Saroglia, M.; Galatà, G.; De Santis, R.; Fillo, S.; Luca, V.; Faggioni, G.; D'Amore, N.; Regalbuto, E.; Salvatori, P.; et al. Magnetic beads combined with carbon black-based screen-printed electrodes for COVID-19: A reliable and miniaturized electrochemical immunosensor for SARS-CoV-2 detection in saliva. *Biosens. Bioelectron.* **2021**, *171*, 112686. [CrossRef]
30. Ameku, W.A.; Provance, D.W.; Morel, C.M.; De-Simone, S.G. Rapid Detection of Anti-SARS-CoV-2 Antibodies with a Screen-Printed Electrode Modified with a Spike Glycoprotein Epitope. *Biosensors* **2022**, *12*, 272. [CrossRef]
31. Liv, L.; Yener, M.; Coban, G.; Can, S.A. Electrochemical biosensing platform based on hydrogen bonding for detection of the SARS-CoV-2 spike antibody. *Anal. Bioanal. Chem.* **2022**, *414*, 1313–1322. [CrossRef]
32. Souza, D.d.; Machado, S.A.S.; Avaca, L.A. Square wave voltammetry. Part I: Theoretical aspects. *Química Nova* **2003**, *26*, 81–89. [CrossRef]
33. Chen, A.; Shah, B. Electrochemical sensing and biosensing based on square wave voltammetry. *Anal. Methods* **2013**, *5*, 2158–2173. [CrossRef]
34. Laborda, E.; Molina, A.; Martínez-Ortiz, F.; Compton, R.G. Electrode modification using porous layers. Maximising the analytical response by choosing the most suitable voltammetry: Differential Pulse vs Square Wave vs Linear sweep voltammetry. *Electrochim. Acta* **2012**, *73*, 3–9. [CrossRef]
35. Uslu, B.; Ozkan, S.A. Electroanalytical Methods for the Determination of Pharmaceuticals: A Review of Recent Trends and Developments. *Anal. Lett.* **2011**, *44*, 2644–2702. [CrossRef]
36. Gupta, V.K.; Jain, R.; Radhapyari, K.; Jadon, N.; Agarwal, S. Voltammetric techniques for the assay of pharmaceuticals–a review. *Anal. Biochem.* **2011**, *408*, 179–196. [CrossRef]
37. Khan, M.Z.H.; Harkin-Jones, E. Effect of ITO surface properties on SAM modification: A review toward biosensor application. *Cogent Eng.* **2016**, *3*, 1170097. [CrossRef]
38. Yang, L.; Li, Y. AFM and impedance spectroscopy characterization of the immobilization of antibodies on indium-tin oxide electrode through self-assembled monolayer of epoxysilane and their capture of Escherichia coli O157:H7. *Biosens. Bioelectron.* **2005**, *20*, 1407–1416. [CrossRef] [PubMed]
39. Ozmen, M.; Can, K.; Ersoz, M. Immobilization of albumin on indium-tin oxide (ITO) surface via isocyanate linkage. *J. Electroanal. Chem.* **2009**, *633*, 228–234. [CrossRef]
40. Gundogdu, A.; Aydin, E.B.; Sezginturk, M.K. A novel electrochemical immunosensor based on ITO modified by carboxyl-ended silane agent for ultrasensitive detection of MAGE-1 in human serum. *Anal. Biochem.* **2017**, *537*, 84–92. [CrossRef] [PubMed]
41. Yagati, A.K.; Lee, T.; Min, J.; Choi, J.W. Electrochemical performance of gold nanoparticle-cytochrome c hybrid interface for H_2O_2 detection. *Colloids Surf. B Biointerfaces* **2012**, *92*, 161–167. [CrossRef]
42. Canbaz, M.C.; Sezginturk, M.K. Fabrication of a highly sensitive disposable immunosensor based on indium tin oxide substrates for cancer biomarker detection. *Anal. Biochem.* **2014**, *446*, 9–18. [CrossRef]
43. Rao, X.; Guyon, C.; Ognier, S.; Da Silva, B.; Chu, C.; Tatoulian, M.; Hassan, A.A. High density gold nanoparticles immobilized on surface via plasma deposited APTES film for decomposing organic compounds in microchannels. *Appl. Surf. Sci.* **2018**, *439*, 272–281. [CrossRef]
44. El-Said, W.A.; Al-Bogami, A.S.; Alshitari, W. Synthesis of gold nanoparticles@reduced porous graphene-modified ITO electrode for spectroelectrochemical detection of SARS-CoV-2 spike protein. *Spectrochim. Acta A Mol. Biomol. Spectrosc.* **2022**, *264*, 120237. [CrossRef] [PubMed]
45. Erdem, A.; Senturk, H.; Yildiz, E.; Maral, M. Impedimetric Detection Based on Label-Free Immunoassay Developed for Targeting Spike S1 Protein of SARS-CoV-2. *Diagnostics* **2022**, *12*, 1992. [CrossRef] [PubMed]

46. Kim, J.; Jeong, S.; Sarawut, S.; Kim, H.; Son, S.U.; Lee, S.; Rabbani, G.; Kwon, H.; Lim, E.K.; Ahn, S.N.; et al. An immunosensor based on a high performance dual-gate oxide semiconductor thin-film transistor for rapid detection of SARS-CoV-2. *Lab Chip* **2022**, *22*, 899–907. [CrossRef]
47. Chang, H.; Jiang, M.; Zhu, Q.; Liu, A.; Wu, Y.; Li, C.; Ji, X.; Gong, L.; Li, S.; Chen, Z.; et al. A novel photoelectrochemical immunosensor based on TiO_2@Bi_2WO_6 hollow microspheres and Ag_2S for sensitive detection of SARS-CoV-2 nucleocapsid protein. *Microchem. J.* **2022**, *182*, 107866. [CrossRef]
48. Gong, J.; Zhang, T.; Luo, T.; Luo, X.; Yan, F.; Tang, W.; Liu, J. Bipolar silica nanochannel array confined electrochemiluminescence for ultrasensitive detection of SARS-CoV-2 antibody. *Biosens. Bioelectron.* **2022**, *215*, 114563. [CrossRef]
49. Hwang, D.-K.; Misra, M.; Lee, Y.-E.; Baek, S.-D.; Myoung, J.-M.; Lee, T.I. The role of Ar plasma treatment in generating oxygen vacancies in indium tin oxide thin films prepared by the sol-gel process. *Appl. Surf. Sci.* **2017**, *405*, 344–349. [CrossRef]
50. Sypabekova, M.; Hagemann, A.; Rho, D.; Kim, S. Review: 3-Aminopropyltriethoxysilane (APTES) Deposition Methods on Oxide Surfaces in Solution and Vapor Phases for Biosensing Applications. *Biosensors* **2022**, *13*, 36. [CrossRef]
51. Drobysh, M.; Liustrovaite, V.; Baradoke, A.; Rucinskiene, A.; Ramanaviciene, A.; Ratautaite, V.; Viter, R.; Chen, C.-F.; Plikusiene, I.; Samukaite-Bubniene, U.; et al. Electrochemical determination of interaction between SARS-CoV-2 spike protein and specific antibodies. *Int. J. Mol. Sci.* **2022**, *23*, 6768. [CrossRef]
52. Rahmati, Z.; Roushani, M.; Hosseini, H.; Choobin, H. An electrochemical immunosensor using SARS-CoV-2 spike protein-nickel hydroxide nanoparticles bio-conjugate modified SPCE for ultrasensitive detection of SARS-CoV-2 antibodies. *Microchem. J.* **2021**, *170*, 106718. [CrossRef] [PubMed]
53. Drobysh, M.; Ramanavicius, A.; Baradoke, A. Polyaniline-based electrochemical immunosensor for the determination of antibodies against SARS-CoV-2 spike protein. *Sci. Total Environ.* **2023**, *862*, 160700. [CrossRef]
54. Liustrovaite, V.; Drobysh, M.; Ratautaite, V.; Ramanaviciene, A.; Rimkute, A.; Simanavicius, M.; Dalgediene, I.; Kucinskaite-Kodze, I.; Plikusiene, I.; Chen, C.-F.; et al. Electrochemical biosensor for the evaluation of monoclonal antibodies targeting the N protein of SARS-CoV-2 virus. *Sci. Total Environ.* **2024**, *924*, 171042. [CrossRef] [PubMed]
55. Samper, I.C.; Sanchez-Cano, A.; Khamcharoen, W.; Jang, I.; Siangproh, W.; Baldrich, E.; Geiss, B.J.; Dandy, D.S.; Henry, C.S. Electrochemical Capillary-Flow Immunoassay for Detecting Anti-SARS-CoV-2 Nucleocapsid Protein Antibodies at the Point of Care. *ACS Sens.* **2021**, *6*, 4067–4075. [CrossRef]
56. Yakoh, A.; Pimpitak, U.; Rengpipat, S.; Hirankarn, N.; Chailapakul, O.; Chaiyo, S. Paper-based electrochemical biosensor for diagnosing COVID-19: Detection of SARS-CoV-2 antibodies and antigen. *Biosens. Bioelectron.* **2021**, *176*, 112912. [CrossRef] [PubMed]
57. Fattahi, A.; Afaghi, P.; Ghandi, K. Catalysis on Nanostructured Indium Tin Oxide Surface for Fast and Inexpensive Probing of Antibodies during Pandemics. *Catalysts* **2021**, *11*, 191. [CrossRef]
58. Wang, R.; Wang, S.; Guo, W.; Zhang, T.; Kang, Q.; Wang, P.; Zhou, F.; Yang, L. Flow injection analysis coupled with photoelectrochemical immunoassay for simultaneous detection of anti-SARS-CoV-2-spike and anti-SARS-CoV-2-nucleocapsid antibodies in serum samples. *Anal. Chim. Acta* **2023**, *1280*, 341857. [CrossRef]